Sedimentology (2004) **51,** 39–51 doi: 10.1046/j.1365-3091.2003.00609.x

A simple model for the prediction of the deflation threshold shear velocity of dry loose particles

W. M. CORNELIS and D. GABRIELS
Department of Soil Management and Soil Care, International Centre for Eremology, Ghent University, Coupure links 653, B-9000 Gent, Belgium (E-mail: wim.cornelis@UGent.be)

ABSTRACT

A very important parameter in aeolian equations is the deflation threshold shear velocity, which quantifies the instant of particle motion. In this paper, a simple model is presented for the prediction of the threshold shear velocity of dry loose particles. It has the same functional form as the widely used models of Bagnold (1941) and Greeley & Iversen (1985), but differs in its treatment of the so-called threshold parameter. As the new expression was based on the moment balance equation used by Greeley & Iversen, it includes a function for the aerodynamic forces, including the drag force, the lift force and the aerodynamic moment force, and a function for the interparticle forces. The effect of gravitation is incorporated in both functions. However, rather than using an implicit function for the effect of the aerodynamic forces as in the Greeley & Iversen model, a constant aerodynamic coefficient was introduced. From consideration of the van der Waals' force between two particles, it was also shown that the function for the interparticle cohesion force is inversely proportional to the particle diameter squared. The model was calibrated on data reported by Iversen & White (1982). The new expression compared, at least for terrestrial conditions, very well with the Greeley & Iversen model, although it is much simpler. It was finally validated with data from wind-tunnel experiments on different fractions of dune sand and sandy loam soil aggregates. The soil aggregates were treated as individual particles with a density equal to their bulk density. The good agreement between observations and predictions means that, when predicting mass transport of particles above a given soil, minimally dispersed particle-size distributions should be considered rather than the granulometric composition of the soil.

Keywords Deflation, threshold, wind erosion, wind tunnel.

INTRODUCTION

Deflation is the blowing away of soil particles by wind. Particles start to move only if the aerodynamic destabilizing forces exceed the stabilizing forces that keep the particles together. Once the wind erosion process has started, particles will also be detached as a result of impact forces caused by the collisions that occur when settling particles hit the surface. The initiation of particle movement is generally quantified by means of the threshold shear velocity u_{*t}. This is the minimal shear velocity required to initiate deflation of soil particles. In other words, for a given wind velocity and surface roughness, particles will be set in motion once the shear velocity u_* exceeds the threshold shear velocity u_{*t}.

The threshold shear velocity u_{*t} of soils depends on many factors such as soil texture, surface roughness and crust formation, aggregate-size distribution, salt and organic matter content, moisture conditions, vegetation, gustiness of the wind, etc. The expressions that are discussed in this paper predict the deflation threshold for soils with uniform and more or less spherical particles spread loosely over a bare and air-dry surface and, hence, they define the lower limit of u_{*t} for a given soil type (Shao & Lu, 2000). For multiple-sized

soils, Shao *et al.* (1996) and Shao (2000) assumed that the dependence of the mass transport on u_* and u_{*t} for one particle-size range is not significantly altered by the presence of other particle sizes. The total saltation mass transport rate Q_s (kg m^{-1} s^{-1}) for a given soil can then be calculated by weighted integration of the saltation mass transport rate $\tilde{Q}_s(d_s)$ for particle sizes d_s (m) in the sand-size range ($d_1 < d_s < d_2$) (Shao *et al.*, 1996):

$$Q_s = \int_{d_1}^{d_2} \tilde{Q}(d_s) p(d_s) \mathrm{d}d_s \qquad (1)$$

where $p(d_s)$ is the mass fraction of particles with diameters ranging between d and $d + \mathrm{d}d$, d_1 is the particle diameter (m) at the fringe between dust and sand (and calculated from the fall velocity of the particle), and d_2 is the diameter (m) of the largest particles that can be transported under a given shear velocity. The saltation mass transport $\tilde{Q}_s(d_s)$ can be predicted from equations proposed by Owen (1964):

$$\tilde{Q}_s(d_s) = 0 \qquad \text{for } u_* < u_{*t},$$

$$\tilde{Q}_s(d_s) = C\frac{\rho_f}{g} u_*(u_*^2 - u_{*t}^2) \qquad \text{for } u_* \geq u_{*t} \qquad (2)$$

where u_* is the shear velocity (m s^{-1}), u_{*t} is the threshold shear velocity (m s^{-1}), which is a function of particle diameter d_s, C is a dimensionless proportionality constant, ρ_f is the fluid density (kg m^3), and g is the gravitational acceleration (m s^{-2}). Transport of suspended material can be predicted in a similar way. The total suspension mass transport Q_{su} of dust particles of all sizes ($0 < d_d < d_1$), induced by bombardment of sand particles of all sizes can be written as (Shao *et al.*, 1996):

$$Q_{su} = \int_{d_1}^{d_2} \int_0^{d_1} \tilde{Q}_{su}(d_d, d_s) p(d_d) p(d_s) \mathrm{d}d_d \mathrm{d}d_s. \qquad (3)$$

The suspension mass transport $\tilde{Q}_{su}(d_d, d_s)$ of dust particles of size d_d (m) induced by saltation bombardment of sand particles of size d_s is (Shao *et al.*, 1996):

$$\tilde{Q}_{su}(d_d, d_s) = \frac{2}{3}\frac{\rho_s}{\rho_f}\frac{\beta_b \gamma g}{u_{*t}^2}\tilde{Q}_s(d_s) \qquad (4)$$

where ρ_s is the particle density (kg m^{-3}), β_b is an empirical bombardment parameter (m) and g is a dimensionless parameter depending on take-off and impact velocities of saltating particles. Eqs (2) and (4) clearly illustrate the importance of accurate estimations of u_{*t} in order to predict mass transport of soil particles.

In the literature, three main theories are described for the initiation of particle movement. Bagnold (1941) considered only a horizontal drag force and the gravitational force on individual particles. Chepil (1958, 1959, 1961) introduced a vertical lift force as an additional force to the drag and gravitational forces. Both theories are only applicable for sand particles >200 and 150 μm respectively. In the 1970s and 1980s, Greeley, Iversen, Pollack and White (see, e.g. Iversen *et al.*, 1976a,b; Iversen & White, 1982) extended, in the framework of a NASA planetary exploration programme for Mars, Venus and Earth, the model of Bagnold (1941) for particles <200 μm and for particle densities and fluid densities other than, respectively, those of quartz and the terrestrial atmosphere. They also considered an aerodynamic moment force and an interparticle cohesion force. Their modifications led to rather complex implicit functions that can only be solved iteratively. A summary of the work by Greeley, Iversen, Pollack and White is found in Greeley & Iversen (1985). The implicit Greeley & Iversen (1985) functions were simplified by Marticorena & Bergametti (1995) and recently by Shao & Lu (2000). The Greeley & Iversen (1985) equations are used in wind erosion models such as WEAM (Shao *et al.*, 1996).

In this paper, a new expression for u_{*t} that has a much simpler functional form than the Greeley & Iversen (1985) equations is presented. It is based on considerations of the different forces that act on particles as they are subjected to wind, and its parameters were derived from least-squares analysis of the Iversen & White (1982) data. The new expression is compared with the Greeley & Iversen (1985) expressions and with the modifications by Marticorena & Bergametti (1995) and Shao & Lu (2000). It is finally validated on data obtained from wind-tunnel experiments on sand particles and sandy loam aggregates.

THEORY

A particle resting on a surface bed and exposed to a fluid stream experiences several forces: a drag force F_D, a lift force F_L, an aerodynamic moment force F_M, the gravitational force F_G and an interparticle cohesion force F_{Ip} (Iversen *et al.*, 1976b) (see Fig. 1).

According to Bagnold (1941), the horizontal drag force F_D (N) caused by the air flow on the particle is proportional to the surface shear stress τ_0 (N m^{-2}) and hence to the shear velocity u_*, which is defined as $u_* = \sqrt{(\tau_0/\rho_f)}$. Iversen *et al.* (1976b) used

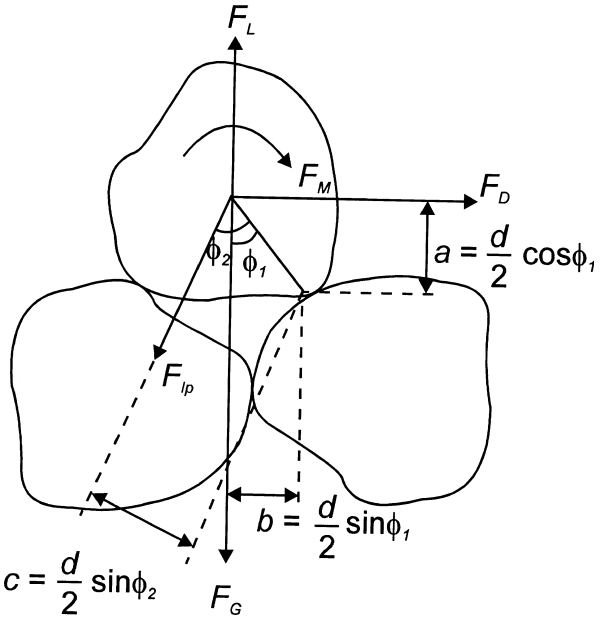

Fig. 1. Forces acting on a particle at rest subjected to an air current, including the horizontal drag force F_D, the lift force F_L, the aerodynamic moment force F_M, the gravitational force F_G and the interparticle force F_{Ip}; a, b and c are moment arm lengths, and ϕ_1 and ϕ_2 are the angles at rest.

expressions similar to Bagnold's for the drag force F_D and the aerodynamic moment force F_M (N), which were based on solutions of Stokes' approximation to the Navier–Stokes equation for viscous flow at low Reynolds numbers (Goldman *et al.*, 1967; O'Neill, 1968). Iversen *et al.* (1976b) also introduced a lift force F_L (N) by obtaining a first-order correction to the Stokes' approximation for small Reynolds numbers (Saffman, 1965). The aerodynamic forces can therefore be written as:

$$F_D = K_F \rho_f u_{*t}^2 d^2, \tag{5}$$

$$F_M = K_M \rho_f u_{*t}^2 d^2, \tag{6}$$

$$F_L = K_L \rho_f u_{*t}^2 d^2 \tag{7}$$

where K_F, K_M and K_L are dimensionless proportionality constants. These coefficients are functions of the threshold Reynolds number $Re_t = \frac{u_{*t} d}{\nu}$, where ν is the kinematic viscosity ($m^2\ s^{-1}$).

The gravitational force F_G (N) on a particle submerged in a fluid can be represented by:

$$F_G = K_G(\rho_s - \rho_f) g d^3 \tag{8}$$

where K_G is a dimensionless proportionality constant ($= \pi/6$ for ideally spherical, smooth particles).

The interparticle force results from cohesion between individual particles. It results from electrostatic force bonding, van der Waals' force bonding and bonding caused by moisture, including adsorbed layer bonding (adhesion forces) and liquid bridge bonding (capillary forces) (Harnby, 1992). The resulting interparticle force is affected by particle shape, particle roughness, particle size, packing density, soil mineralogy and the presence of bonding agents such as organic matter, salts and moisture. As the objective of this paper was to develop a new expression to predict the threshold shear velocity of dry material, only electrostatic and van der Waals' forces will be considered here. The effect of adsorbed layer bonding and liquid bridge bonding due to moisture is discussed by Cornelis *et al.* (2004a,b,c). Electrostatic and van der Waals' forces between solid particles result in long-range interactions and not only act on the area of contact between the particles, but also contribute considerably to the overall adhesive forces as a result of their appreciable magnitudes extending outside the actual interface (Yariv & Cross, 1979). Short-range interactions resulting from various types of chemical bonds as well as hydrogen bonds across the interface occur only to a small extent (Yariv & Cross, 1979) and are neglected here.

The electrostatic force $F_{Ip,e}$ (N) (or Coulomb force) occurs when two solids in rubbing contact will charge each other electrostatically. The surface charge density, which is relatively uniform over the complete surface for non-conducting bodies, will largely determine the force of attraction between particles (Harnby, 1992). Provided the amount of charges between two spherical particles equals q_1 and q_2 (C), the (Coulomb) electrostatic force of two particles can be written as (Adamson & Gast, 1997):

$$F_{Ip,e} = \frac{1}{4\pi\varepsilon_0\varepsilon} \frac{q_1 q_2}{(d + x_d)^2} \tag{9}$$

where ε_0 is the dielectrical constant of vacuum ($C^2\ N^{-1}\ m^{-2}$), ε is the dimensionless dielectrical constant of the medium and x_d the distance between the particles (m). As q is proportional to d_2, $F_{Ip,e}$ should be a function of d_2. The electrostatic force may be attractive or repulsive, depending on the charge sign of the two particles.

The van der Waals' force $F_{Ip,vdW}$ (N) (or London dispersion force) is responsible for the attraction of molecules without permanent dipoles. The extension of the theory of van der Waals' attractive forces from the atomic or microscopic scale to bulk powders on the macroscopic scale was first carried

out in the 1950s by Lifshitz (Harnby, 1992). Because of the additivity of the atomic forces, the van der Waals' attraction between macroscopic particles is much stronger than that between gaseous atoms and molecules, and it increases with particle size (Hobbel, 1988). For two parallel flat plates of thickness d at a distance x_d from each other, the van der Waals' force of attraction between the plates is given by (Iwata *et al.*, 1988):

$$F_{Ip,vdW_{plate-plate}} = \frac{A_H}{48\pi x_d}\left[\frac{1}{\left(\frac{x_d}{2}\right)^2} + \frac{1}{\left(\frac{x_d}{2}+d\right)^2} - \frac{2}{\left(\frac{x_d}{2}+\frac{d}{2}\right)^2}\right] \quad (10)$$

where A_H is the Hamaker constant (J), named after its developer (Hamaker, 1937). Note that the Hamaker 'constant' A_H varies somewhat with the particle separation. This effect was first recognized by Casimir & Polder (1948) and was treated later by Lifshitz (Harnby, 1992) through quantum field theory. When $d >> x_d$, Eq. (10) becomes (Adamson & Gast, 1997):

$$F_{Ip,vdW_{plate-plate}} = \frac{A_H}{12\pi x_d^3}. \quad (11)$$

The van der Waals' force of attraction between a sphere and a flat surface can be expressed as (Adamson & Gast, 1997):

$$F_{Ip,vdW_{plate-sphere}} = \frac{A_H}{6x_d}\left\{\frac{1}{\left(1+\frac{x_d}{d}\right)^2-1} + \frac{1}{\left(1+\frac{x_d}{d}\right)^2} + 2\ln\left[1-\frac{1}{\left(1+\frac{x_d}{d}\right)^2}\right]\right\} \quad (12)$$

For two spherical particles, the van der Waals' force becomes (Adamson & Gast, 1997):

$$F_{Ip,vdW_{sphere-sphere}} = \frac{1}{2}F_{Ip,vdW_{plate-sphere.}} \quad (13)$$

When $d \gg x_d$, Eq. (12) can be written as (Adamson & Gast, 1997):

$$F_{Ip,vdW_{plate-sphere}} = \frac{A_H}{12x_d^2}d. \quad (14)$$

As soil particles are mainly a mixture of spheres and plates, and the electrostatic forces are several degrees of magnitude smaller than the van der Waals' forces (Harnby, 1992), it can be assumed that F_{Ip} is proportional to d. When considering A_H and x_d as being constant, Eqs (11), (13) and (14) can be simplified as:

$$F_{Ip} = K_{Ip}d^n \quad (15)$$

where K_{Ip} is a proportionality coefficient (N m^{-n}) and $n = 1$. However, it is rather doubtful that x_d is a constant for all particle-size ranges, as it will depend not only on particle geometry, but also on the degree of compaction.

At the instant of particle motion, the destabilizing forces F_D, F_L and F_M will exceed the stabilizing forces F_G and F_{Ip}, and the particle will pivot about a downstream point of contact. At the instant of deflation, the moments about the pivot point are balanced (Fig. 1):

$$F_D a + F_M d = (F_G - F_L)b + F_{Ip}c \quad (16)$$

where a, b and c are moment arm lengths (m). When substituting Eqs (5–8) and Eq. (15) into Eq. (16) and with $a = a_1\,d$, $b = b_1\,d$ *and* $c = c_1\,d$, the threshold shear velocity u_{*t} becomes:

$$u_{*t} = A\sqrt{\frac{\rho_s - \rho_f}{\rho_f}gd} \quad (17)$$

where

$$A = \sqrt{\frac{b_1K_G}{a_1K_D + b_1K_L + K_M}}\sqrt{1 + \frac{c_1K_{Ip}}{b_1K_G(\rho_s - \rho_f)gd^{3-n}}} \quad (18)$$

or

$$A = A'F(Re_t)G(d) \quad (19)$$

is the dimensionless threshold parameter. The first term of the right-hand part in Eq. (19), $A'F(Re_t)$, is a function accounting for the dependence of the aerodynamic drag on the Reynolds number Re_t and the second, $G(d)$, is a cohesion term and function of particle diameter. Greeley & Iversen (1985) reported the following equation for $G(d)$:

$$G(d) = \sqrt{1 + \frac{0.00610^{-4}}{\rho_s g d^{2.5}}} \quad (20)$$

assuming that the particles are perfectly spherical ($K_G = \pi/6$) and that the angle at rest ϕ_1 is about $\pi/5$ ($b_1 \approx 1/4$) and by applying linear regression of $\frac{c_1K_{Ip}}{b_1K_Gd^{3-n}}$ data against $\left[A^2\left(\frac{b_1K_G}{a_1K_D+b_1K_L+K_M}\right)^{-1} - 1\right]\rho_s g$ data which were obtained from measurements in a series of wind-tunnel experiments with a range of particle sizes, particle densities and wind-tunnel pressures.

By dividing A by the cohesion function $G(d)$, the function $A'\,F(Re_t)$ was isolated, and non-linear multiple regression resulted in the following equations (Greeley & Iversen, 1985):

$$A'F(Re_t) = 0.2\frac{1}{\sqrt{1+2.5Re_t}} \quad \text{for } 0.03 \le Re_t \le 0.3,$$

$$A'F(Re_t) = 0.129\frac{1}{\sqrt{1.928Re_t 0.092 - 1}}$$

$$\text{for } 0.3 \le Re_t \le 10,$$

$$A'F(Re_t) = 0.120\sqrt{1+0.0858\exp[-0.0617(Re_t-10)]}$$

$$\text{for } Re_t \ge 10. \qquad (21)$$

As Eq. (21) is an implicit function – Re_t is related to u_{*t} and A – which can only be solved iteratively, Marticorena & Bergametti (1995) used an analytical expression for Re_t:

$$Re_t = 1331(100\ d)^{1.56} + 0.38. \qquad (22)$$

Equation (22) was developed by determining numerically (d, u_{*t}) data pairs and by computing the corresponding Re_t values for terrestrial conditions, i.e. with $\rho_f = 1{\cdot}23\ 10^{-3}$ Mg m^{-3} and $\rho_s = 2{\cdot}65$ Mg m^{-3}.

As an alternative for Eq. (21), $A'\,F(Re_t)$ could be expressed as a function of fluid density ρ_f, particle density ρ_s and particle diameter d, as these parameters will determine the value of Re_t. When computing $A'\,F(Re_t)$ using Eq. (21) for the different planetary conditions including those on Mars, Earth and Venus as reported in Iversen & White (1982), relatively good fits to the Iversen & White (1982) data were obtained when simplifying $A'\,F(Re_t)$ to (see Fig. 2):

$$A'F(Re_t) = \sqrt{A_1\left(1+A_2\frac{\rho_s}{\rho_f}\right)\left(1+A_3\frac{1}{d}\right)} \qquad (23)$$

where A_1 and A_2 are dimensionless regression coefficients and A_3 is a regression coefficient expressed in metres. Note that the values of $A'F(Re_t)$ in Fig. 2 are probably overpredicted, as the Greeley & Iversen (1985) cohesion term is a function of $d^{-2{\cdot}5}$ (see Eq. 20) rather than the theoretical d^{-2} (see Eq. 18 with $n = 1$).

However, the question arises if, for terrestrial conditions, the aerodynamic coefficients K_D, K_L and K_M cannot be treated as constants rather than as a function of Re_t. By linear regression of the cohesionless term $A'\,F(Re_t)$ in Eq. (19) against Re_t values between 0·03 and 0·3, Iversen & White (1982) found that $K_D + 2{\cdot}45$, $K_M = 4{\cdot}65$ and $K_L = 32{\cdot}8\ Re_t$. According to Chepil (1958), K_L is proportional to K_D (being 0·85 K_D). Equation (18) can therefore be simplified, and the model we propose is:

$$A = \sqrt{A_4\left[1+A_5\frac{1}{(\rho_s-\rho_f)gd^{3-n}}\right]} \qquad (24)$$

where

$$A_4 = \frac{b_1K_G}{a_1K_D + b_1K_L + K_M} \qquad (25)$$

and

$$A_5 = \frac{c_1K_{Ip}}{b_1K_G} \qquad (26)$$

are constants. Equation (24) will be also tested here with $n \neq 1$ and with $A_4 = A_1\left(1+A_2\frac{\rho_s}{\rho_f}\right)\left(1+A_3\frac{1}{d}\right)$ (see Eq. 23). This model (Eq. 24) is much simpler than the expressions proposed by Greeley & Iversen (1985) (Eqs 19–21).

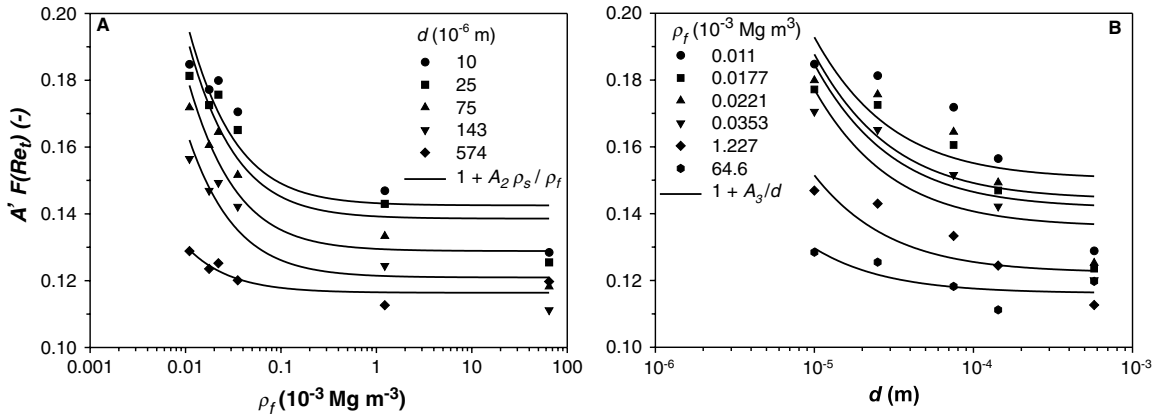

Fig. 2. The aerodynamic factor $A'F(Re_t)$ vs. fluid density ρ_f at different particle diameters d (A) and vs. particle diameter d at different fluid densities ρ_f (B). The data are from Iversen & White (1982).

Recently, Shao & Lu (2000) reanalysed the Iversen & White (1982) data within the particle-size range 50–1800 mm and found:

$$A'F(Re_t) = \sqrt{0.0123} \tag{27}$$

$$G(d) = \sqrt{1 + A_6 \frac{1}{\rho_s g d^2}} \tag{28}$$

where the values of A_6 range between $1{\cdot}65 \times 10^{-4}$ and 5×10^{-4} N m^{-1}. In general, Shao & Lu (2000) recommend an A_6 value of around 3×10^{-4} N m^{-1}. Note that the functional form of the expression of Shao & Lu (2000) is similar to the model that is proposed in this paper.

It should be noted here that Eq. (17) is identical to the well-known Bagnold (1941) expression. It is worthwhile to recall Bagnold's theory briefly, as it forms the basis for the aerodynamic term $A'F(Re_t)$ in Eq. (19). According to Bagnold, the shear velocity at which deflation of soil particles starts is a function of the size and density of those particles only. Cohesion forces were not considered. The parameter A is, as with many numerical coefficients in fluid dynamics, only constant over limited ranges of the flow regime as defined by the Reynolds number. In most cases, the flow regime is fully turbulent. However, when considering small-scale flow over and round the individual particles on the surface, the flow is not always fully turbulent, which depends on Re_t. Bagnold reported that, when $Re_t > 3{\cdot}5$, the particle behaves as an isolated obstacle in the path of the fluid and throws off a chain of tiny eddies from its lee face. Moreover, under these conditions, an exposed particle lying by itself above its neighbours can carry the whole of the drag on the area it occupies, together with most of that on the surrounding shielded area, even when this is 20 times the projected area of the particle (Colebrook & White, 1937, cited by Bagnold, 1941). For particles >200 μm (fine dune sand), that is for $Re_t > 3{\cdot}5$ (according to Bagnold's observations, u_{*t} is about 0·22 m s^{-1} for fine dune sand), A is constant and equal to 0·1 in air. Bagnold reasoned that, when $Re_t < 3{\cdot}5$, that is when the particle diameter, the threshold velocity or both are smaller than those for fine dune sand, the individual particles cease to shed little eddies of their own, and a semi-viscous, non-turbulent layer of the fluid clings around them. The drag, instead of being carried by the few more exposed particles, is distributed more or less evenly over the whole surface. Consequently, a relatively greater drag is required to set the first particles in motion. As a result, the value of the coefficient A for air begins to rise when the particle size d falls below about 200 μm. As Bagnold worked with dune sand only, he was not able to prove his theory experimentally. If it turns out that $A'F(Re_t)$ can be treated as a constant, which is proposed here, this would mean that the above effect is negligible compared with the effect of the interparticle forces.

Finally, it must be emphasized that Eq. (19) is only valid for the initial phase of particle detachment. At the initiation of deflation, the particles are set in motion as a result of aerodynamic forces. Once deflation has started, and particles are transported in the air stream, the impact forces of the settling particles when they hit the surface will contribute to the deflation of new particles. After a certain period of time, particle impact will take over the deflation function from the fluid forces. As particle impact receives a great part of its energy from the air current above the surface, the new threshold to maintain erosion will be considerably lower than the initial threshold. Bagnold termed those threshold parameters impact threshold and fluid threshold respectively. For $Re_t > 3{\cdot}5$, it was found that $A = 0{\cdot}08$ for the impact threshold. Anderson & Haff (1988) reported similar values.

MATERIALS AND METHODS

The parameter values of the model that is proposed here were determined by a non-linear least-squares analysis on the data reported by Iversen & White (1982). These data were obtained from experiments in the Iowa State University boundary-layer wind tunnel located at Ames, IA, USA. The working pressure of the tunnel was about 100 kPa (one atmosphere, that is at terrestrial conditions). Material ranging from tea to lead with different particle sizes and particle densities was used. Particle size ranged from 12 to 1290 μm, and particle density from 0·21 to 11·35 Mg m^{-3}. Air density ρ_f was $1{\cdot}226 \times 10^{-3}$ Mg m^{-3}, and kinematic viscosity ν was $14{\cdot}65 \times 10^{-6}$ m^2 s^{-1}. In order to study particle motion at fluid densities appropriate for the planet Mars, the Martian Surface Wind Tunnel (MARSWIT) was build at the NASA Ames Research Center, Moffet Field, CA, USA. This tunnel is capable of attaining atmospheric pressures from 100 kPa down to 0·38 kPa. The data that were obtained from experiments in MARSWIT were added to the data from the ISU wind

tunnel and led to Eqs (20) and (21). From the experimental results given in Iversen & White (1982), it was clear that some scatter exists on the low-density data, especially at $Re_t > 0{\cdot}1$. Repeatability was relatively poor for those experiments. As wind erosion on Earth where $Re_t > 0{\cdot}3$ (for particles >12 μm) is being considered, only the more reliable one-atmosphere data were used in this study.

The non-linear multiple regressions that were used in order to find the values of the parameters in Eq. (24) were executed by applying a quasi-Newton minimizing method (Press *et al.*, 1992). This procedure finds the parameter values that give the best fit between the model and the data, that is that minimize the sum of squared differences between observed and predicted values of the dependent variable. In obtaining the parameters in Eq. (24), two different approaches can be applied. In a first approach, the objective function to be minimized is:

$$SSE_{u*_t} = \sum_{i=1}^{N} \left[u_{*t_i} - \hat{u}_{*_t}(d_i, \rho_{s_i}, A_M)\right]^2 \qquad (29)$$

where u_{*t_i} is the observed threshold shear velocity, $\hat{u}_{*_t}(d_i, \rho_{s_i}, A_M)$ is the predicted threshold shear velocity value at corresponding d_i and ρ_{s_i} values, A_M is a 6×1 matrix containing the values for A_1–A_5 and n depending on the model used, and $i = 1 \ldots N$, with N the number of observations. This procedure has been followed by Shao & Lu (2000). As Eq. (29) includes the term $\sqrt{\frac{\rho_s - \rho_f}{\rho_f f} g d}$, better fits can be expected at extreme ρ_s and d values, in comparison with an objective function such as:

$$SSE_A = \sum_{i=1}^{N} \left[A_i - \hat{A}(d_i, \rho_{s_i}, A_M)\right]^2 \qquad (30)$$

where A_i is the observed threshold parameter and $\hat{A}(d_i, \rho_{s_i}, A_M)$ is the predicted threshold parameter at corresponding d_i and ρ_{s_i}. The latter approach is, however, more logical as it is the threshold parameter A that contains the unknown coefficients A_M. Both approaches were considered in this study. The two approaches are evaluated by comparing the residuals as a function of d and ρ_s. The observed A values were calculated from Eq. (17). The model that is proposed here with the parameters derived from curve fitting will be referred to as model1 CG. This model includes two coefficients: A_4 and A_5 ($n = 1$). Equation (24) will also be tested with $n \neq 1$, where n is determined from curve fitting, and with $A_4^{0.5}$ from Eq. (23). These models are referred to as model2 CG and model3 CG respectively.

Once A_M was obtained, the validity of the fitted models as well as the model of Greeley & Iversen (1985) (model GI), the model of Marticorena & Bergametti (1995) (model MB) and the model of Shao & Lu (2000) (model SL) was tested by analysing the sum of squared errors, and the Akaike Information Criterion *AIC*, which is often used for model discrimination tests (Hippel, 1981):

$$AIC = N\left[\log(2\pi) + \log\left(\frac{SSE}{N-p}\right) + 1\right] + p \qquad (31)$$

where p is the number of parameters in the model. Note that, in the SL model, A_6 was taken to be 3×10^{-4} N m $^{-1}$as recommended by Shao & Lu (2000).

The new model was validated for dune sand particles and for soil aggregates through wind-tunnel experiments at the International Centre for Eremology (ICE), Ghent University, Belgium. The particle-size ranges that were used included 100–200 μm, 200–500 μm and 50–500 μm for the dune sand and 50–100 μm, 100–200 μm, 200–300 μm and 300–500 μm for the soil aggregates. The aggregates were taken from a sandy loam soil on an agricultural field near Melle (Belgium), whereas the sand was collected from the Belgian coastal dunes (Bredene). The particle density was 2·65 Mg m^{-3} and 1·47 Mg m^{-3} for the dune sand and the sandy loam aggregates respectively. Note that the sandy loam aggregates are considered here as solid particles with a particle density equal to their bulk density. Table 1 summarizes some of the physico-chemical characteristics of both sediments, as well as their fully dispersed particle-size distributions. The particle-size distributions were determined by the pipette method (Gee & Bauder, 1986). Organic matter measurements were based on the Walkley & Black (1934) method, and the electrical conductivity at 25 °C was measured on a saturated extract with Pl electrodes.

The ICE wind tunnel is a closed-circuit blowing-type wind tunnel with a 12 m long, 1·2 m wide and 3·2 m high working section (Gabriels *et al.*, 1997). The boundary layer was set at about 0·60 m using a combination of spires and roughness elements (Cornelis, 2002). The sand and soil samples were placed in $0{\cdot}95 \times 0{\cdot}40 \times 0{\cdot}02$ m trays, which were located at a distance $x =$ 6·00 m downwind from the entrance of the wind-tunnel working section. The sample surface

Table 1. Fully dispersed particle-size distribution and physico-chemical properties of the two sediments used in the experiments.

Sediment	Clay* content (%)	Silt content (%)	Sand content (%)	OM† content (%)	$CaCO_3$ content (%)	EC_e (dS m^{-1})
Dune sand	1·3	0·3	98·4	0·0	3·3	0·72
Sandy loam	6·7	30·3	63·0	2·0	0·0	0·43

*Clay 0–2 μm, silt 2–50 μm, sand 50–2000 μm.
†OM is organic matter, EC_e is the electrical conductivity at 25 °C measured on a saturated extract.

was smoothed and levelled to the test section false floor by drawing a straight edge across the sample surface. To ensure wind profile equilibrium with the roughness of the sample surface, the test section was covered with commercially available emery paper with the same roughness length as the surface of the sample, as determined experimentally from measured wind velocity profiles.

Wind velocity u_z was monitored at a 1-Hz frequency with 16-mm vane probes mounted at heights z of 0·025 m, 0·096 m, 0·170 m, 0·256 m and 0·377 m located at a downwind distance $x = 5{\cdot}85$ m and a width $y = 0{\cdot}60$ m. Shear velocity u_* of the surface was calculated from the mean of wind velocity readings using a least-squares fit to the well-known Prandtl–von Kármán logarithmic law:

$$\bar{u}_z = \frac{u_*}{\kappa} \ln \frac{z}{z_0}, \tag{32}$$

where $\bar{u}_z$ is mean wind velocity (m s^{-1}) at height z (m), κ is the von Kármán constant (= 0·4) and z_0 is the roughness length (m).

The initiation of particle movement was determined by continuously recording particle transport with a saltiphone, placed at $x = 6{\cdot}85$ m, $y = 0{\cdot}60$ m and $z = 0{\cdot}035$ m, at shear velocities that are fluctuating around the threshold value. The saltiphone is an acoustic sediment sensor that records the number of saltating particles that bounce against a microphone at a frequency of 0·1 Hz. The microphone is installed in a stainless steel tube. A potentiometer amplifies the high frequencies caused by the impact of sand particles, whereas it attenuates the low frequencies that characterize the noise caused by wind. Each particle impact produces a pulse that is cut off after 1 ms. A detailed description of the saltiphone is given by Spaan & van den Abeele (1991). The impact energy of the soil aggregates smaller than 200 μm was, however, too low to be recorded by the saltiphone. In those two cases, particle entrainment was determined by means of a neon–helium laser beam (Logie, 1982).

RESULTS AND DISCUSSION

First, it was tested which curve fitting approach – minimizing the objective function (Eq. 29) or (Eq. 30) with $n = 1$ and A_4 from Eq. (25) – performed best. In Fig. 3, the residuals of A and u_{*t} are plotted against d and ρ_s for both approaches. Both approaches gave worst fits at the lowest d values (when considering A; see Fig. 3A) and at the highest ρ_s values (when considering u_{*t}; see Fig. 3D). As could be expected, it is only at the very high particle densities (8·94 Mg m^{-3} and 11·35 Mg m^{-3}) that minimizing SSE_{u*t} resulted in better fits. For all other cases, minimizing SSE_A gave the best results. The coefficients of the CG models that are proposed here are therefore based on the latter approach. However, the means of the squared residuals obtained from both approaches were not significantly different at the 0·2 level.

Estimates of the parameters of the three 'new' models, obtained as described above, are given in Table 2. Table 3 gives the *SSE*, *AIC*, R^2 values for all the tested models. When mutually comparing the 'new' models, it seems that model3 CG performs the best, followed by model2 CG. The decrease in *SSE* is associated with a decrease in *AIC*. The reduction in *SSE* thus compensates for the additional parameters in the model, meaning that the increase in likelihood (lower *SSE*) is more important than the reduction in simplicity of the model (in terms of the number of parameters). The means of the squared residuals are, however, not significantly different at the 0·1 level.

When analysing the residuals of u_{*t} as a function of diameter and particle density, highest residuals are observed at the highest particle densities (8·94 Mg m^{-3} and 11·35 Mg m^{-3}), particularly in the case of model1 CG (Fig. 4). These high particle densities correspond to the very low and the very high particle diameters of the data set (12 μm,

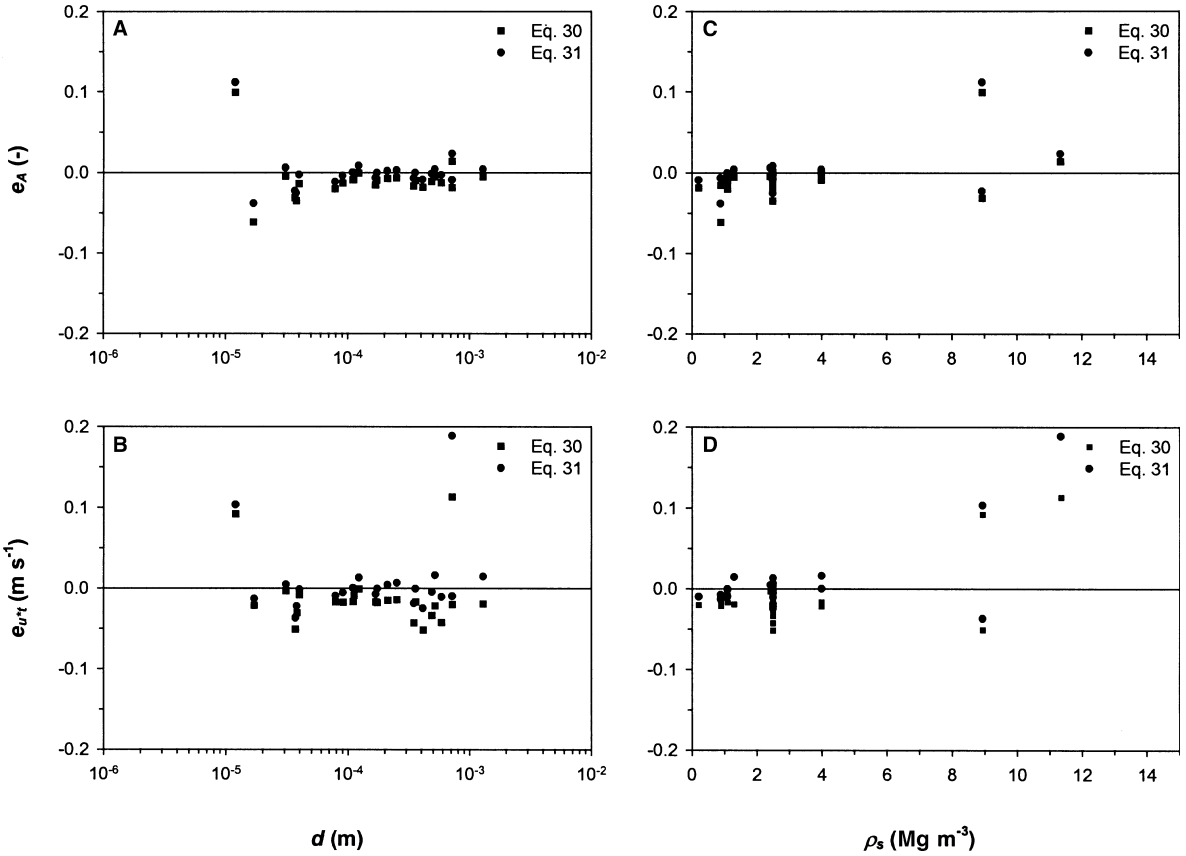

Fig. 3. The residuals e_A and e_{u^*t} vs. particle diameter d in (A) and (B), respectively, and vs. particle density ρ_s in (C) and (D), respectively, for model1 CG as obtained from minimizing Eqs (30) and (31).

37 μm and 720 μm). For almost all other data, model1 CG shows the lowest residuals and, thus, model1 CG performs best if those extremely high particle densities are omitted (see Table 4). For most applications in wind erosion, particle density will be lower than those extreme values. Therefore, model1 CG can be considered as the best of the 'new' models, at least for terrestrial conditions. For non-terrestrial conditions, model3 CG, which considers the aerodynamic term $A'F(Re_t)$ as a function of fluid density and particle diameter (and hence Re_t), rather than treating it as a constant, will probably perform better. The proposed parameters were, however, not tested for conditions with higher or lower fluid densities than those of the calibration data set.

The very good performance of the proposed two-parameter model could indicate that it is reasonable, at least for terrestrial conditions, to treat the cohesionless term in Eq. (19) as a constant. This would mean that the effect of drag being more evenly shared on a bed of only fine

Table 2. Coefficient values of the three 'new' models.

Model	Model1 CG	Model2 CG	Model3 CG
A_1 (–)	–	–	0·010 (0·001; < 0·0001)
A_2 (10^{-6})	–	–	85·761 (0·000; 0·2036)
A_3 (10^{-6} m)	–	–	1·498 (0·000; 0·0011)
A_4 (–)	0·013 (0·002; < 0·0001)*	0·015 (0·002; < 0·0001)	–
A_5 (10^{-6} N m^{-n})	169·500 (0·000; < 0·0001)	7·073 (0·000; 0·4791)	177·420 (0·000; < 0·0001)
n (–)	1	0·719 (0·122; < 0·0001)	1†

*The values between parentheses are the standard error and the level of significance.
†This value was fixed and not determined by curve fitting.

Table 3. Sum of squared errors *SSE*, determinant R^2 and Akaike Information Criterion *AIC* of the tested models.

Model	*SSE* (m s^{-1})	R^2 (–)	*AIC* (–)
Model1 CG	0·050	0·943	−18·2
Model2 CG	0·031	0·966	−21·9
Model3 CG	0·012	0·986	−29·8
Model GI	0·031	0·965	−12·1
Model MB	0·043	0·952	−1·6
Model SL	0·085	0·904	−12·7

particles than on a bed with coarse ones is not very important, which was also suggested by Cooke *et al.* (1993). This is also illustrated in Fig. 2, which shows that the range of 'overestimated' A' $F(Re_t)$ values is relatively narrow for relatively high fluid densities as on Earth. If one assumes that the aerodynamic coefficients K_D, K_L and K_M are constants and $K_L = 0{\cdot}85$ K_D, $K_M = 0{\cdot}445$ K_D (Chepil, 1958), $K_G = \pi/6$ (which is the case for spheres; Iversen & White, 1982) and $\phi_1 = \pi/5$ (Greeley & Iversen, 1985), it follows from Eq. (25), with $A_4 = 0{\cdot}013$ (see Table 2), that K_D should be around 14. This value is close to 15·42 obtained by Coleman & Ellis (1976).

To check whether the proposed equation for the interparticle forces, i.e. Eq. (15) with $n = 1$, is acceptable, K_{Ip} was calculated from the curve fitted A_5. With $K_G = \pi/6$, $\phi_1 = \pi/5$ and $\phi_2 = \pi/4$, K_{Ip} thus becomes $7{\cdot}4 \times 10^{-5}$ N m^{-1}. This value can be compared with the constants in Eq. (14). As van der Waals' forces are several degrees of magnitude larger than electrostatic forces (Harnby, 1992), the latter can be omitted here. Tabor & Winterton (1968, 1969) and Israelachvili & Tabor (1972) measured $10{\cdot}7 \times 10^{-20}$ J and $13{\cdot}5 \times 10^{-20}$ J, respectively, as the Hamaker constant for mica. For silica, Israelachvili (1992) and Hough & White (1980) give values of $6{\cdot}5 \times 10^{-20}$ J and $6{\cdot}55 \times 10^{-20}$ J respectively. The Hamaker constant in Eq. (14) was set here at 10×10^{-20} J, a value that is applicable to many materials. The average distance between two particles l should be of the order of magnitude of 100 Å so that that F_{Ip}, calculated with Eqs (14) and (15) would give a similar result. Such a distance is a typical value for fine-textured soils (van Olphen, 1977).

To illustrate the relative importance of the different forces, their moments are plotted as a function of particle diameter under terrestrial conditions and for particles with a density of 2·65 Mg m^{-3} (Fig. 5). To avoid any assumption about the angle of repose or the shape of the particles, the moments are divided by b_1 K_G (see legend to Fig. 5). The destabilizing aerodynamic forces are grouped together, and their moment factors are calculated for $u_* = 0{\cdot}25$ m s^{-1} and $u_* = 0{\cdot}50$ m s^{-1}. Figure 5 clearly illustrates that the effect of cohesion becomes more important than the weight effect of the particles once their diameter becomes lower than about 80 μm. If the shear velocity is 0·25 m s^{-1}, the aerodynamic effect exceeds the effect of the stabilizing forces when the particle diameter is between about 30 μm and 200 μm and, consequently, particles of this size will be blown away at such a shear velocity. If $u_* = 0{\cdot}50$ m s^{-1}, particles with diameter between about 8 μm and 900 μm will be susceptible to deflation. This is in full agreement with the model1 CG predictions.

In Fig. 6, the observed data are plotted together with the data predicted with the proposed model (model1 CG) and the GI model, the MB model and

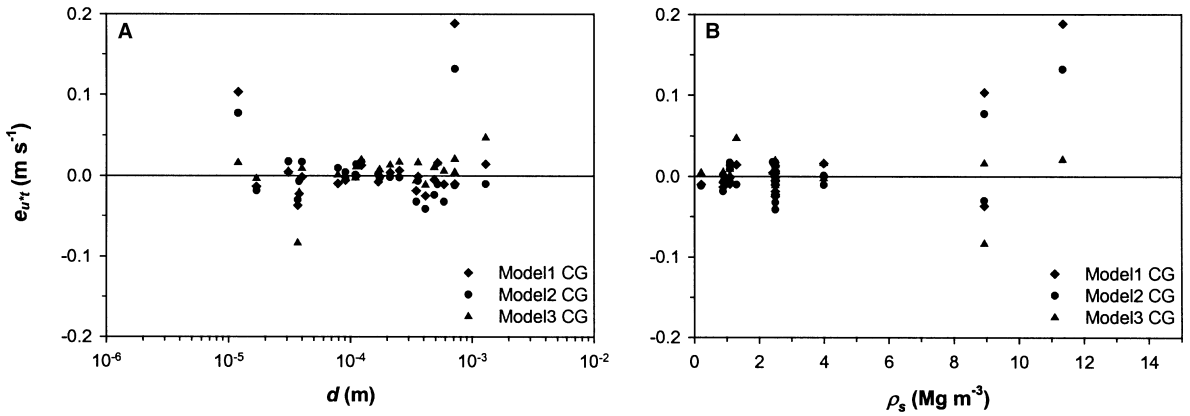

Fig. 4. The residuals e_{u^*t} vs. particle diameter d (A) and vs. fluid density ρ_f (B) for model1 CG, model2 CG and model3 CG.

Table 4. As Table 3 but when omitting the high-density data (8·94 Mg m^{-3} and 11·35 Mg m^{-3}).

Model	*SSE* (m s^{-1})	R^2 (–)	*AIC* (–)
Model1 CG	0·003	0·997	−48·4
Model2 CG	0·006	0·993	−38·3
Model3 CG	0·005	0·995	−39·9
Model GI	0·007	0·992	−27·4
Model MB	0·008	0·991	−19·1
Model SL	0·034	0·962	−22·3

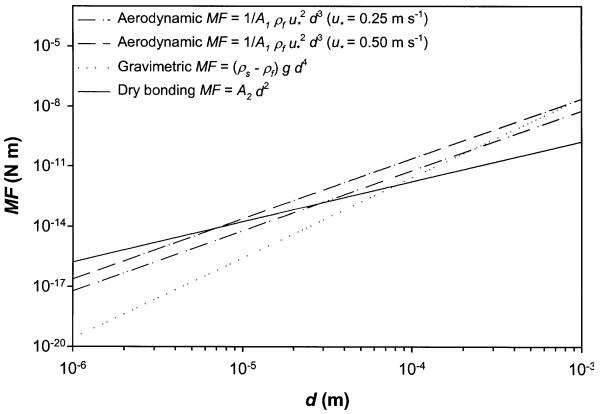

Fig. 5. The different moment factors *MF* acting on a particle at rest vs. particle diameter *d*.

the SL model. All models seem to perform very accurately (see also Tables 3 and 4). The least accurate is the Shao & Lu (2000) simplification. It has to be mentioned that these authors only considered particles >50 μm. It is particularly at these small particle sizes that the SL model shows the highest deviations from the observations. In analysing the work of Zimon (1982), who measured cohesive forces acting upon small powder particles, Shao (2000) suggested the use of a log-normal probabilistic distribution of the threshold shear velocity for fine particles, rather than a single value. However, more wind-tunnel research is needed to confirm this hypothesis. On the other hand, the work of Iversen *et al.* (1976a,b), Iversen & White (1982) and Greeley & Iversen (1985) indicates that loose fine (dust) particles with a diameter smaller than say 50 μm – a size that is often used as the limit between dust and sand – can be lifted up by wind shear only and, hence, suspension does not necessarily have to be induced by bombardment of impacting particles in saltation, as is often believed. This has important implications for defining d_d in Eqs (3) and (4).

In Fig. 7, the two-parameter model that is presented here is validated against data for dune sand and for sandy loam soil aggregates that were obtained through wind-tunnel experiments in this study. Figure 8 illustrates how the saltiphone can be used to determine the threshold shear velocity for a given particle diameter. In the case of soil aggregates with a bulk density of 1·47 Mg m^{-3} and an average diameter of 250 μm, particles start to be blown away once the shear velocity u_* exceeds a value of about 0·23 m s^{-1}. As shear velocity increases, the number of impacts rises as well. Figure 7 shows that the threshold shear velocities predicted with the proposed model agree very well with the observed data. This means that soil aggregates can be treated as individual particles with a density equal to their bulk density. Prediction of mass transport for a given soil using Eqs (2) and (4) should therefore be based on minimally

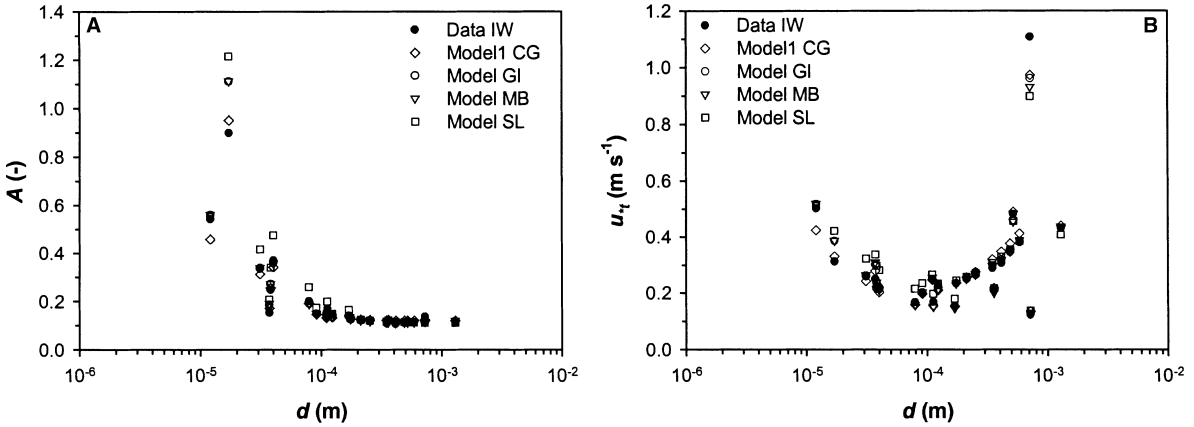

Fig. 6. The threshold parameter *A* (A) and the threshold shear velocity u_{*t} (B) vs. particle diameter *d*: the observed Iversen & White (1982) data (IW), the model1 of this study (CG), the Greeley & Iversen (1985) model (GI), the Marticorena & Bergametti (1995) model (MB) and the Shao & Lu (2000) model (SL).

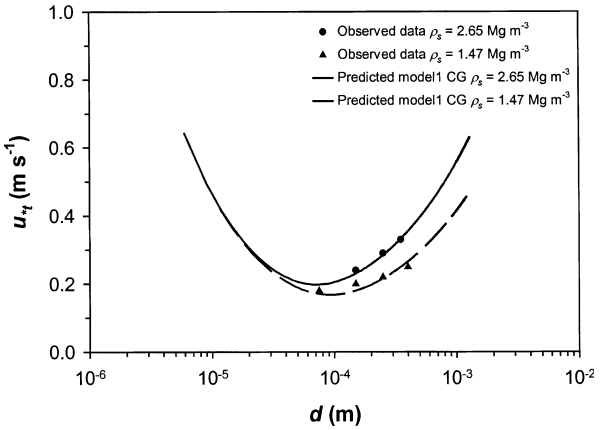

Fig. 7. Observed (this study) and predicted (model1 CG) threshold shear velocities u_{*t} vs. particle diameter d.

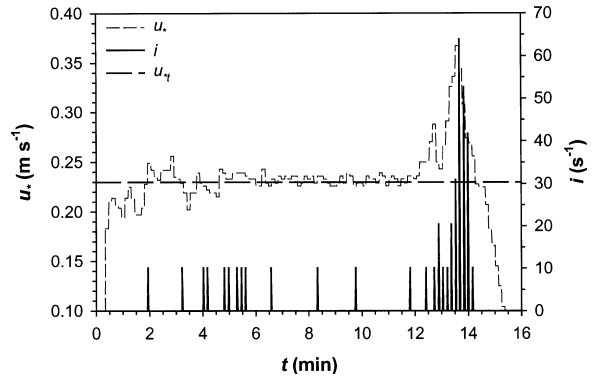

Fig. 8. Example of shear velocity u_* and particle flux i vs. time t plot for soil aggregates with a mean diameter of 250 μm and a bulk density $\rho_b = 1{\cdot}47$ Mg m^{-3}, used to determine the threshold shear velocity u_{*t}.

dispersed particle-size distributions, rather than on fully dispersed ones.

SUMMARY AND CONCLUSIONS

A simple model is proposed to predict the threshold shear velocity u_{*t} for dry loose soil particles as a function of their diameter d. It is developed by reanalysing the data of Iversen & White (1982) as reported in literature. The model is based on the balance of moments that act on soil particles at the instant of particle motion. It includes a function for the aerodynamic forces, including the drag force F_D, the lift force F_L and the aerodynamic moment force F_M and a function for the interparticle forces. The effect of gravitation is incorporated in both functions. The analysis revealed that it is reasonable, at least for terrestrial conditions, to consider the function for the aerodynamic forces as a constant rather than to treat it as a function of the threshold Reynolds number Re_t. From consideration of the van der Waals' forces between two particles, it was shown that the effect of the interparticle (cohesion) force on the deflation threshold was inversely proportional to the particle diameter squared. The aerodynamic constant and the cohesion proportionality constant of the proposed two-parameter model were determined by non-linear least-squares regression, and their values were 0·013 and $1{\cdot}695 \times 10^{-4}$ N m^{-1} respectively. Two alternative models, with three and four parameters, were considered as well, but did not perform considerably better than the two-parameter model.

When the moments of the aerodynamic forces are calculated from the aerodynamic constant that was determined by curve fitting and from values for the aerodynamic factors K_D, K_L and K_M that were found in the literature, they agreed very well. The same was true when comparing the interparticle force F_{Ip} calculated from the cohesion constant with the van der Waals' force that was calculated from theory, including a value for the Hamaker constant that was found in the literature. Taking an average particle distance of 100 Å, both forces agreed very well.

When comparing the presented model with three other models found in the literature that were based on the same data set, it came out that the new model performed as accurately, although the model is much simpler.

Finally, the threshold shear velocity was determined for different-sized dune sand and soil aggregates using wind-tunnel experiments. The observed values agreed very well with the predicted ones. The soil aggregates were treated as individual particles with a density equal to their bulk density. The good correlation means that, when predicting mass transport of particles above a given soil, minimally dispersed particle-size distributions should be considered rather than the granulometric composition of the soil.

REFERENCES

Adamson, A.W. and **Gast, A.P.** (1997) *Physical Chemistry of Surfaces*, 6th edn. John Wiley & Sons, New York.

Anderson, R.S. and **Haff, P.K.** (1988) Simulation of eolian saltation. *Science*, **241,** 820–823.

Bagnold, R.A. (1941) *The Physics of Blown Sand and Desert Dunes*. Chapman & Hall, London.

Casimir, H.B.G. and **Polder, D.** (1948) The influence of retardation on the London-van der Waals forces. *Phys. Rev.*, **73,** 360–372.

Chepil, W.S. (1958) The use of evenly spaced hemispheres to evaluate aerodynamic forces on a soil surface. *Trans. Am. Geophys. Union*, **39,** 397–403.

Chepil, W.S. (1959) Equilibrium of soil grains at the threshold of movement by wind. *Soil Sci. Soc. Am. Proc.*, **24,** 143–145.

Chepil, W.S. (1961) The use of spheres to measure lift and drag on wind-eroded soil by wind. *Soil Sci.*, **60,** 305–320.

Coleman, N.L. and **Ellis, W.M.** (1976) *Model Study of the Drag Coefficient of a Streambed Particle. Proceedings of the 3rd Federal Interagency Sedimentation Conference*, Denver, pp. 4–12.

Cooke, R., Warren, A. and **Goudie, A.** (1993) *Desert Geomorphology*. UCL Press, St Ives.

Cornelis, W.M. (2002) Erosion processes of dry and wet sediment induced by wind and wind-driven rain: a wind-tunnel study. PhD Dissertation, Ghent University.

Cornelis, W.M., Gabriels, D. and **Hartmann, R.** (2004a) A conceptual model to predict the deflation threshold shear velocity as affected by near-surface moisture content. 1. Theory. *Soil Sci. Soc. Am. J.*, (in press).

Cornelis, W.M., Gabriels, D. and **Hartmann, R.** (2004b) A conceptual model to predict the deflation threshold shear velocity as affected by near-surface moisture content. 2. Calibration and verification. *Soil Sci. Soc. Am. J.*, (in press).

Cornelis, W.M., Gabriels, D. and **Hartmann, R.** (2004c) A parameterisation for the threshold shear velocity to initiate deflation of dry and wet sediment. *Geomorphology*. doi:10.1016/j.geomorph.2003.09.004.

Gabriels, D., Cornelis, W.M., Pollet, I., Van Coillie, T. and **Ouessar, M.** (1997) The ICE wind tunnel for wind and water erosion studies. *Soil Techn.*, **10,** 1–8.

Gee, G.W. and **Bauder** (1986) Particle-size analysis. In: *Methods of Soil Analysis, Part 1. Physical and Mineralogical Methods* (Ed. A. Klute), 2nd edn, pp. 383–411. Agronomy Monograph no. 9. ASA-SSSA, Madison, WI.

Goldman, A.J., Cox, R.G. and **Brenner, H.** (1967) Slow viscous motion of a sphere parallel to a plane wall, II. *Chem. Eng. Sci.*, **22,** 653–660.

Greeley, R. and **Iversen, J.D.** (1985) *Wind as a Geological Process on Earth, Mars, Venus and Titan*. Cambridge University Press, Cambridge.

Hamaker, H.C. (1937) The London-van der Waals attraction between spherical particles. *Physica*, **4,** 1058–1072.

Harnby, N. (1992) The mixing of cohesive powders. In: *Mixing in the Process Industries* (Eds N. Harnby, M.F. Edwards and A.W. Nienow), 2nd edn, pp. 79–98. Nienow, Butterworth-Heinemann, Oxford.

Hippel, K.W. (1981) Geophysical model discrimination using the Akaike Information Criterion. *IEEE Trans. Autom. Control*, **AC-26,** 358–378.

Hobbel, E.F. (1988) Cohesion and interparticle forces. PhD Thesis, Technical University Delft, Delft.

Hough, D.B. and **White, L.R.** (1980) The calculation of Hamaker constants from Lifshitz theory with applications to wetting phenomena. *Adv. Colloid Interface Sci.*, **14,** 3–41.

Israelachvili, J.N. (1992) *Intermolecular and Surface Forces*, 2nd edn. Academic Press, San Diego.

Israelachvili, J.N. and **Tabor, D.** (1972) The treatment of van der Waals dispersion forces in the range of 1.5–130 nm. *Proc. R. Soc. London*, **A331,** 19–38.

Iversen, J.D. and **White, B.R.** (1982) Saltation threshold on Earth, Mars and Venus. *Sedimentology*, **29,** 111–119.

Iversen, J.D., Greeley, R. and **Pollack, J.B.** (1976a) Wind blown dust on Earth, Mars and Venus. *J. Atmos. Sci.*, **33,** 2425–2429.

Iversen, J.D., Pollack, J.B., Greeley, R. and **White, B.R.** (1976b) Saltation threshold on Mars: the effect of interparticle force surface roughness, and low atmospheric density. *Icarus*, **29,** 381–393.

Iwata, S., Tabuchi, T. and **Warkentin, B.P.** (1988) *Soil–Water Interactions*. Marcel Dekker, New York.

Logie, M. (1982) Influence of roughness elements and soil moisture on the resistance of sand to wind erosion. *Catena Suppl.*, **1,** 161–174.

Marticorena, B. and **Bergametti, G.** (1995) Modeling the atmospheric dust cycle: 1. Design of a soil-derived dust emission scheme. *J. Geophys. Res.*, **100,** 16415–16416, 430.

O'Neill, M.E. (1968) A sphere in contact with a plane wall in a slow linear shear flow. *Chem. Eng. Sci.*, **23,** 1293–1298.

van Olphen, H. (1977) *An Introduction to Clay Colloid Chemistry: for Clay Technologists, Geologists, and Soil Scientists*. John Wiley & Sons, New York.

Owen, P.R. (1964) Saltation of uniform grains in air. *J. Fluid Mech.*, **20,** 225–242.

Press, W.H., Flannery, W.T., Teukolsky, S.A. and **Vetterling, B.P.** (1992) *Numerical Recipes in C.* Cambridge University Press, New York.

Saffman, P.G. (1965) The lift on a small sphere in a slow shear flow. *J. Fluid Mech.*, **22,** 385–400.

Shao, Y. (2000) Physics and modelling of wind erosion. Atmospheric and Oceanographic Sciences Library, 23. Kluwer Academic Publishers, Dordrecht.

Shao, Y. and **Lu, H.** (2000) A simple expression for wind erosion threshold friction velocity. *J. Geophys. Res.*, **105,** 22,437–22,432, 443.

Shao, Y., Raupach, M.R. and **Leys, J.F.** (1996) A model for predicting aeolian sand drift and dust entrainment on scales from paddock to region. *Aust. J. Soil Res.*, **34,** 309–342.

Spaan, W.P. and **van den Abeele, G.D.** (1991) Wind borne particle measurements with acoustic sensors. *Soil Techn.*, **4,** 51–63.

Tabor, D. and **Winterton, R.H.S.** (1968) Surface forces: direct measurement of normal and retarded van der Waals forces. *Nature*, **219,** 1120–1121.

Tabor, D. and **Winterton, R.H.S.** (1969) The direct measurement of normal and retarded van der Waals forces. *Proc. R. Soc. London*, **A321,** 435–450.

Walkley, A. and **Black, I.A.** (1934) An examination of the Degtjareff method for determining soil organic matter and a proposed modification of the chromic acid titration method. *Soil Sci.*, **37,** 29–38.

Yariv, S. and **Cross, H.** (1979) *Geochemistry of Colloid Systems*. Springer-Verlag, Berlin.

Zimon, A. (1982) *Adhesion of Dust and Powder*. Consultants Bureau, New York.

Manuscript received 13 May 2002;
revision accepted 19 September 2003.